Available online at www.sciencedirect.com
ScienceDirect
Trans. Nonferrous Met. Soc. China 34(2024) 336−346
Transactions of Nonferrous Metals Society of China
www.tnmsc.cn

Recovery of Li and Fe from spent lithium iron phosphate using organic acid leaching system

Ya-hui WANG[1], Ji-jun WU[1,2], Guo-chen HU[1], Wen-hui MA[1,2]

1. Faculty of Metallurgical and Energy Engineering, Kunming University of Science and Technology, Kunming 650093, China;
2. National Engineering Laboratory of Vacuum Metallurgy, Kunming University of Science and Technology, Kunming 650093, China

Received 29 July 2022; accepted 5 April 2023

Abstract: The valuable metals, lithium and iron, were recovered from spent $LiFePO_4$ cathode powder by hydrometallurgy, and the recycled products were used as raw materials for the preparation of lithium iron phosphate. By the optimization of the leaching process parameters, the leaching efficiency of Li reached 96.56% at pyruvic acid concentration of 3.0 mol/L, volume of H_2O_2 of 2 mL, solid-to-liquid ratio of 0.1 g/mL, reaction temperature of 80 °C, and reaction time of 20 min. The leached residue was characterized by XRD, XPS, and FE-SEM coupled with EDS, and the results showed that the leached residue was $FePO_4$ with an Fe/P molar ratio of 0.974. After adjusting the pH of the leaching solution to 12.0 and stirring for 2 h at 80 °C, the recovery of Li from the leaching solution was enabled by in-situ precipitation in the form of Li_3PO_4 with a purity of 96.5 wt.%. The reaction kinetic data of Li leaching using the pyruvic acid/H_2O_2 solution were fit to the Avrami model with R^2>0.95. The low activation energy of the Li leaching process indicated that diffusion step limited the reaction rate during the leaching process.
Key words: spent $LiFePO_4$; pyruvic acid; leaching kinetics; Avrami model; lithium ion batteries

1 Introduction

In recent years, China has made major strategic commitments to achieve carbon peaking and carbon neutrality by 2030 and 2060, respectively, by developing and using clean energy. Central to these commitments is the automobile industry, which has become a national strategic emerging industry and has entered a stage of rapid development, especially in the electric vehicle (EV) market [1,2]. Currently, most lithium-ion batteries used in electric vehicles are lithium iron phosphate (LIP) rather than other lithium-containing metal salts, such as lithium nickel manganese cobalt oxide (NMC) or lithium cobalt oxide (LCO). LIP batteries are advantageous because they have high working voltage, high energy density and long cycle life, and do not exhibit a memory effect [3]. Therefore, the rapid growth of LIP utilization has demanded the development of environmentally sustainable and efficient methods to recycle spent LIP batteries after their service life [4]. Spent LIP batteries cannot be directly discarded or buried because they would pollute the soil and underlying groundwater with metal elements [5], resulting in not only valuable wasted metal resources but also serious environmental pollution [6].

The recovery methods to valuable cathodic metal materials from spent LIP batteries mainly involves pyrometallurgical [7] and hydrometallurgical [8−11] processes, the latter of which have a significantly higher recovery rate and can enable a better separation of impurities [12,13].

Corresponding author: Ji-jun WU, Tel: +86-13888411653, E-mail: dragon_wu213@126.com
DOI: 10.1016/S1003-6326(23)66402-7

As for hydrometallurgy, inorganic [14−16] or organic [17−19] acids were used to leach the valuable metal ions from the spent electrode materials, and oxidants are added to the leaching solution to perform oxidation−reduction reactions to recover the metallic elements from the solution. Some researchers have selectively leached Li from spent $LiFePO_4$ by adding an aqueous solution of $(NH_4)_2S_2O_8$ [20] or $K_2S_2O_8$ [21] as the oxidant, but these solutions are highly corrosive. Therefore, an acid with high leaching efficiency and friendly environment is desired to recover valuable metals from spent $LiFePO_4$ cathode materials by hydrometallurgical method.

Pyruvic acid is more acidic (pK_a=2.49) than formic acid (pK_a=3.75) and acetic acid (pK_a=4.76) but is less acidic than sulfuric acid (pK_{a1}=−2.00), oxalic acid (pK_{a1}=1.22) and phosphoric acid (pK_{a1}=2.12), which are also used as leaching agents. Till now, researchers using organic acid leaching systems have explored selective leaching of lithium. In this study, pyruvic acid was used as the leaching agent to achieve the non-selective leaching of lithium from spent $LiFePO_4$, providing a new idea for metal recovery from spent $LiFePO_4$ cathode materials.

2 Experimental

2.1 Materials

The spent $LiFePO_4$ cathode powder used in the experiment was purchased from BYD Company. The ICP-OES analysis of spent $LiFePO_4$ cathode powder showed that the contents of Li, Fe, C and P were 4.36%, 33.98%, 1.79% and 18.72%, respectively. The XRD diffraction pattern of the spent $LiFePO_4$ cathode powder was consistent with the standard spectrum of $LiFePO_4$ (PDF# 81-1173) (Fig. 1). The other reagents and chemicals used in the experiment, including pyruvic acid (≥70 wt.%), hydrogen peroxide (30 wt.% H_2O_2), and sodium hydroxide (NaOH), were all of analytical grade and were used as obtained without purification.

2.2 Experimental leaching procedure

In a beaker, spent $LiFePO_4$ cathode powder was mixed with ≥70 wt.% aqueous solution of pyruvate, to which 30 wt.% hydrogen peroxide solution in water was slowly added. The beaker was sealed and heated in a constant temperature heated water bath while the solution was stirred magnetically to perform the leaching process. After leaching, the beaker was removed from the water bath, and the solution was immediately filtered. During the filtration, the leaching residue was washed with deionized water 3−5 times to avoid influencing the concentration of the metal in the leaching solution. The leached residue was analyzed after 12 h of drying at 100 °C. The leaching residue was calcined at 600 °C for 4 h to remove the C-containing impurities. To recover the Li from the leaching solution, an solution of NaOH (2 mol/L) was added to the leached solution to adjust the pH and to precipitate the Fe as $Fe(OH)_3$. After filtration of the precipitated $Fe(OH)_3$ to remove them from the leaching solution, the pH of the filtrate was further adjusted to 12.0 with NaOH solution to precipitate the lithium as Li_3PO_4. Figure 2 shows the entire process of recovering the Li (as Li_3PO_4) from the spent $LiFePO_4$ cathode powder.

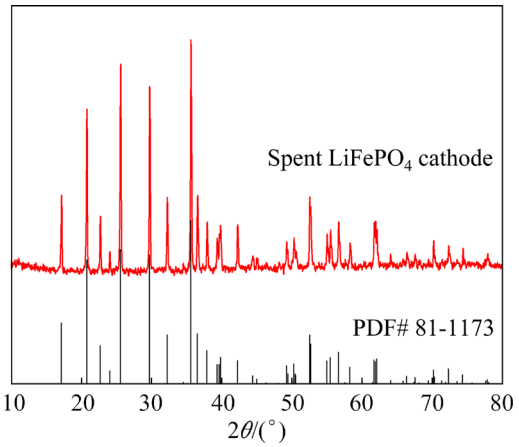

Fig. 1 XRD pattern of spent $LiFePO_4$ cathode powder

To reduce any potential statistical error during the experiment, each experiment was repeated three times. The variance of the Li data was (1±0.06) and that of the Fe data was (3±0.04) during the entire set of experiments. The leaching efficiency of the Li metal was calculated using Eq. (1):

$$\eta=[1-(\omega_2 m_2)/(\omega_1 m_1)]\times 100\% \quad (1)$$

where ω_2 represents the mass fraction (%) of Li and Fe in the leaching slag, ω_1 represents the mass fraction (%) of Li and Fe in the reaction raw material, m_2 represents the mass (g) of the leached residue, m_1 represents the mass (g) of the reaction raw material, and η represents the metal leaching efficiency (%).

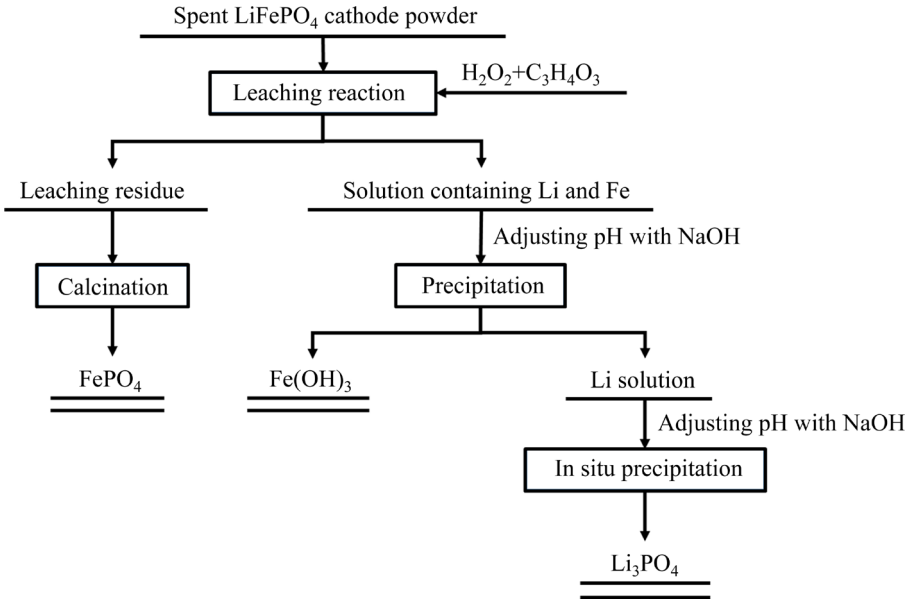

Fig. 2 Process flow of recovering valuable metal from spent $LiFePO_4$ cathode powder

2.3 Characterization

The morphology of the spent $LiFePO_4$ cathode powder and leached slag was characterized by field-emission scanning electron microscopy (FE-SEM, Nova Nano SEM 450, FEI Company, USA) coupled with energy-dispersive X-ray spectroscopy (EDS). The concentrations of Li and Fe in the leaching solution and the content of the metal elements in the leached residue were analyzed by inductively coupled plasma-optical emission spectrometry (ICP-OES, 7700x, USA). The spent $LiFePO_4$ cathode powder, recovered lithium products, and leached residue were characterized by X-ray diffraction (XRD, X'pert^3 Powder, Netherlands). X-ray photoelectron spectroscopy (XPS, PHI 5000 VersaProbe-II, Japan) was used to analyze the phase of the spent $LiFePO_4$ cathode powder and leached residue.

3 Results and discussion

3.1 Optimization of pyruvic acid concentration

The effect of pyruvic acid concentration on the leaching efficiency of Li and Fe was studied, and the results are shown in Fig. 3(a). The leaching experiments were initially performed at a reaction temperature of 80 °C, solid-to-liquid ratio of 0.10 g/mL, volume of 30 wt.% hydrogen peroxide of 2 mL, and reaction time of 120 min. Under these conditions, as the pyruvate concentration increased from 1.0 to 3.5 mol/L, the leaching efficiency of Li increased from 50.78% to 98.24%, the leaching efficiency of Fe increased from 44.55% to 98.55%, and the pH of the leaching solution decreased from 3.1 to 2.0. When the concentration of pyruvate increased from 3 to 3.5 mol/L, the leaching efficiency of Li and Fe increased by only 1.64% and 0.88%, respectively. Therefore, the leaching efficiency of Li and Fe only negligibly increased when the concentration of pyruvic acid increased beyond 3 mol/L. The dramatic rise in leaching efficiency as the concentration of pyruvic acid increased to 3 mol/L was attributed to the acceleration of the reaction between the pyruvic acid and the $LiFePO_4$, causing the lithium to be separated from the $FePO_4$ [17]. Therefore, to achieve as high a leaching efficiency of lithium and waste treatment from $LiFePO_4$ as possible, 3.0 mol/L was selected as the optimal concentration of pyruvic acid.

3.2 Optimization of H_2O_2 volume

Figure 3(b) depicts the influence of the amount of H_2O_2 added on the leaching efficiency of Li and Fe. During these experiments, the reaction temperature was 80 °C, the solid-to-liquid ratio was 0.10 g/mL, the reaction time was 120 min, and the pyruvate concentration was 3.0 mol/L. When no H_2O_2 was added, although the leaching efficiencies of Li and Fe were 95.84% and 94.80%, respectively

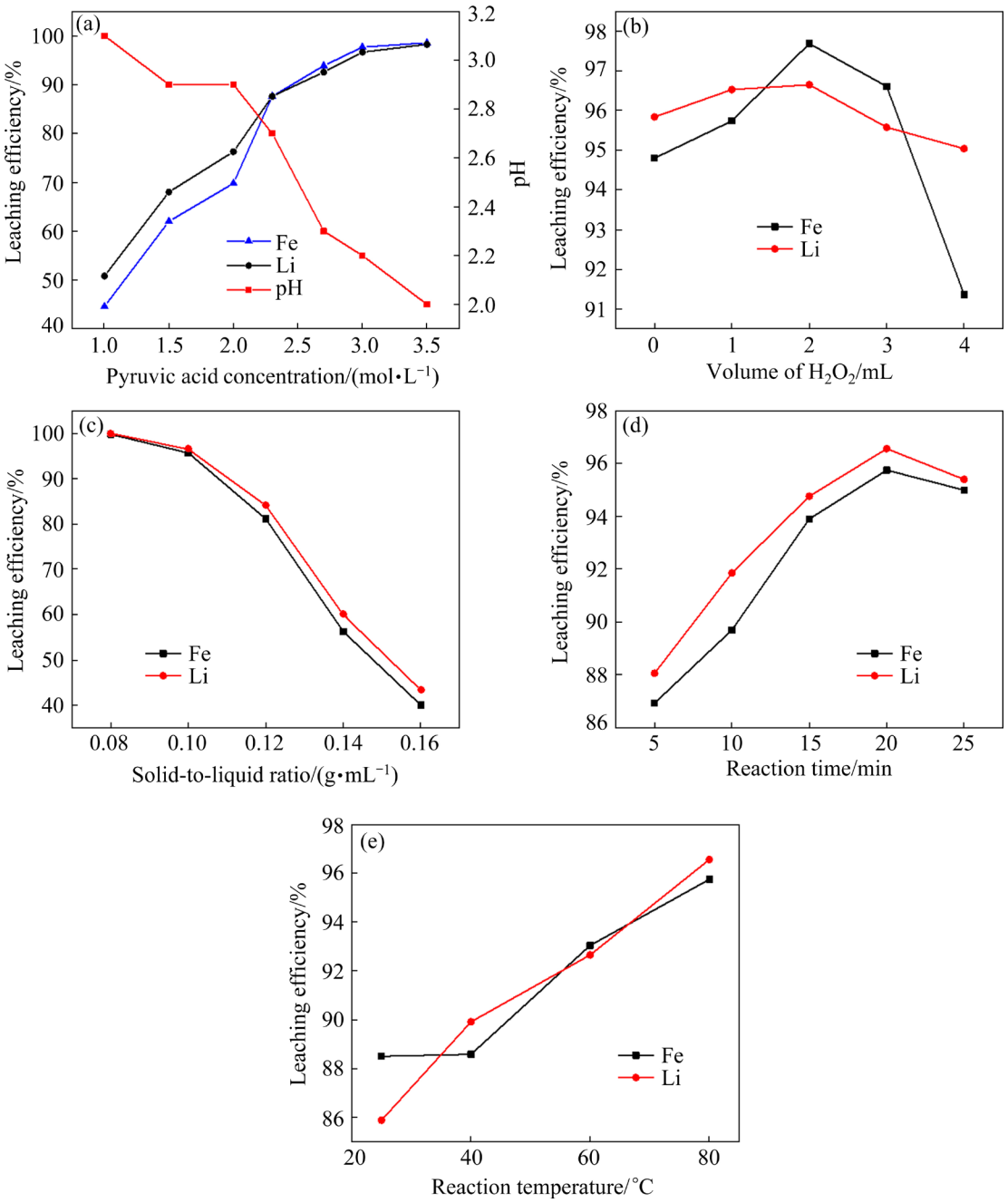

Fig. 3 Effects of different process parameters on leaching efficiency of spent $LiFePO_4$ cathode powder: (a) Pyruvic acid concentration; (b) Hydrogen peroxide volume; (c) Solid-to-liquid ratio; (d) Reaction time; (e) Reaction temperature

(Fig. 3(b)), the Li was not completely leached from the spent powder. When the volume of H_2O_2 increased from 1 to 2 mL, the leaching efficiency of Li and Fe increased to 96.65% and 97.69%, respectively. As the volume of H_2O_2 solution increased, the high concentration of H_2O_2 caused more Fe(II) to be oxidized to Fe(III), enabling a better separation of Li from the $FePO_4$ in the LIP powder. However, when the volume of H_2O_2 exceeded 2 mL, the leaching efficiency of Li and Fe decreased significantly because the redox reactions between H_2O_2 and Fe^{2+} consumed H^+ (Reaction (2)), resulting in a decrease in the concentration of H^+ in solution, thereby reducing the concentration of acid and thus the leaching efficiency. In addition, the H_2O_2 needed to be added slowly during the experiment because the bubbles generated could cause the solution in the reactor to easy overflow if it were added too quickly. Furthermore, more volume of H_2O_2 made the reaction more exothermic, thus producing more heat.

$$2Fe^{2+}+H_2O_2+2H^+\rightarrow 2Fe^{3+}+2H_2O \quad (2)$$

3.3 Optimization of solid-to-liquid ratio

Next, the influence of solid-to-liquid ratio over the range of 0.08−0.16 g/mL on the leaching efficiency of Li and Fe was studied, and the results are shown in Fig. 3(c). As the solid-to-liquid ratio increased from 0.08 to 0.16 g/mL, the leaching efficiency of Li and Fe decreased from 99.98% to 43.31% and from 99.79% to 40.01%, respectively. This change indicated that lower solid-to-liquid ratios manifested higher leaching efficiencies because there was more contact area between the spent $LiFePO_4$ cathode powder and pyruvic acid in the leaching solution when the ratios were lower, which improved Li leaching efficiency [18,22,23]. However, in actual production, a higher solid-to-liquid ratio is usually required to improve production efficiency, which leads to lower leaching efficiencies [24]. To ensure a higher leaching efficiency, 0.1 g/mL was selected as the optimal leaching solid-to-liquid ratio for future experiments.

3.4 Optimization of leaching time and temperature

The effects of the leaching time (5−25 min) and temperature (25, 40, 60, and 80 °C) on the leaching efficiency of Li and Fe were studied, and the results are shown in Figs. 3(d) and (e), respectively. When the reaction time increased from 5 to 20 min, the leaching efficiency of Li increased from 88.06% to 96.56%; however, as the reaction time increased further to 25 min, the leaching efficiency of Li decreased from 96.56% to 95.4% (Fig. 3(d)). Therefore, 20 min was chosen as the optimal reaction time. Furthermore, the leaching efficiency of Li increased as the leaching reaction temperature increased (Fig. 3(e)). When the leaching reaction was run at 80 °C, the highest of the studied temperatures, the leaching efficiency of Li was 96.56%. Since the leaching of metals is endothermic, a higher reaction temperature was more conducive to ensuring a higher leaching efficiency than running the leaching reactions at lower temperature [25]. However, higher temperatures facilitate the evaporation of the solution; therefore, 80°C was chosen as the optimal reaction temperature for future experiments.

It was concluded from the optimization experiments that a pyruvate concentration of 3.0 mol/L, a volume of 30 wt.% H_2O_2 of 2 mL, a solid-to-liquid ratio of 0.1 g/mL, a reaction temperature of 80 °C, and a reaction time of 20 min were the optimal reaction conditions to achieve the most efficient leaching of Li from the $LiFePO_4$. Under these conditions, the leaching efficiencies of Li and Fe were 96.56% and 95.75%, respectively, which indicated that the pyruvic acid leaching system did not exhibit selective leaching (i.e., high leaching efficiency of iron). Therefore, this study differed from other studies that organic acid leaching systems were utilized. In the E−pH diagram of the Li−Fe−P−H_2O system [20], the $LiFePO_4$ phase was stable over the pH range of 1.7−7.2 and electrochemical potential from −0.5 to 0 V. The $FePO_4$ phase was stable over the pH range of 1.7−6.0 and the electrochemical potential of 0−0.75 V. The crystal structure of $LiFePO_4$ consisted of a slightly twisted hexagonal close-packed structure consistent with an orthorhombic lattice system. The tetrahedral PO_4 in the spatial skeleton of the $LiFePO_4$ lattice limited the volume change of the lattice, which affected the deintercalation and ion diffusion of Li^+ ions [23]. The olivine-structured $LiFePO_4$ is considered one of the most ideal cathode materials for lithium-ion batteries. The phase transformation involves a volume decrease (6.81%) as lithium gets rid of the $LiFePO_4$ framework. Therefore, the conversion of Fe(II) to Fe(III) during the delithiation process is vital to ensure the selective leaching of Li from $LiFePO_4$ [18].

H^+ provided by the ionization of pyruvic acid can combine with hydrogen peroxide to form water, which are expressed as Reactions (3) and (4), respectively:

$$CH_3COCOOH(aq)\rightarrow CH_3COCOO^-(aq)+H^+(aq),\ K_a=3.2\times10^{-3} \quad (3)$$

$$H_2O_2+2H^++2e=H_2O,\ \varphi_1^{\ominus}=1.77\ V \quad (4)$$

Furthermore, the reaction of spent $LiFePO_4$ powder, pyruvic acid, and hydrogen peroxide can be expressed by Reaction (5):

$$CH_3COCOOH(aq)+LiFePO_4(s)+1/2H_2O_2(aq)\rightarrow CH_3COCOO^-(aq)+Li^+(aq)+FePO_4(s)+H_2O(l) \quad (5)$$

The spontaneity of the pyruvic acid leaching reaction was analyzed from the perspective of thermodynamics. The standard Gibb's free energy of formation ($\Delta_fG^{\ominus}$) of pyruvate was calculated by approximating the bond enthalpy. The standard molar generation Gibb's free energy ($\Delta_fG^{\ominus}$) values

of reactants $LiFePO_4$, H_2O_2, and $CH_3COCOOH$ were 1480.97, 120.42, and 346.26 kJ/mol, respectively. The standard molar generation Gibb's free energy (Δ_fG^{Θ}) values of the products $FePO_4$, Li^+, H_2O, and CH_3COCOO^- were 1110.14, 293.31, 237.18, and 320.7 kJ/mol, respectively [26]. Thus, the Gibb's free energy (Δ_rG^{Θ}) of the entire leaching process was calculated to be −73.89 kJ/mol; $\Delta_rG^{\Theta}<0$ implies that the reaction is favorable and energy-yielding. These data also indicated that the thermodynamic process must be forward, but the actual reaction needs to consider the dynamics.

3.5 Leaching residue analysis

After optimizing the experimental conditions, the optimal leaching parameters of the spent $LiFePO_4$ cathode powder were determined. Figures 4(a) and (b) show XRD and XPS results of the leached residue, respectively. The XRD diffraction pattern of the leached residue was consistent with the standard spectrum of $FePO_4$ (PDF# 34-0134) and the XPS featured diffraction peak corresponded to Fe^{3+} at the binding energy of 712.2 and 725.9 eV [27]. This indicated that not only was the Fe^{2+} in $LiFePO_4$ oxidized to Fe^{3+} after exposure to H_2O_2 and pyruvate, but also the Fe^{3+} was present in the form of $FePO_4$, which was consistent with previously published studies [28]. Furthermore, the XRD data not only indicated that both the spent $LiFePO_4$ cathode powder and leached slag had orthogonal olivine crystal structures but also confirmed the formation of $FePO_4$ in the leached slag.

FE-SEM was used to study the morphologies of the spent $LiFePO_4$ cathode powder and leached residue. As shown in the SEM images, the spent $LiFePO_4$ cathode powder (Fig. 5(a)) and leached residue (Fig. 5(b)) were very similar and the particles were large in size. In the EDS analysis of the FE-SEM images, a significant amount of C-containing impurities derived from the carbon source of the $LiFePO_4$ battery remained in leached residue after leaching; this was consistent with the results of ICP-OES analysis of the raw materials. From the ICP-OES analysis results, the leaching residue of C content was 38.39%. Because Li is a very light element, the X-ray yield is low, making energy X-ray (EDS) mapping of Li nearly impossible. Therefore, the leached residue was calcined at 600 °C for 4 h to remove C-containing impurities. After calcination, the C content decreased from 38.39% to 0.35%, and the removal rate reached 99.09%. The ICP-OES results of the calcined products are shown in Table 1. The ICP-OES analysis of the calcined products showed that the calculated Fe/P molar ratio of the iron phosphate in the product was 0.974 (the standard is 0.97−0.98). In addition, the concentrations of the trace elements that ultimately affected the reuse of $FePO_4$ were determined; since the contents of impurities were low ($\leq 150\times10^{-6}$ for Al, $\leq 50\times10^{-6}$ for Zn, and $\leq 20\times10^{-6}$ for Ni), it was determined that the treated $FePO_4$ could be used for the synthesis of catalyst and $LiFePO_4$ cathode materials.

3.6 Recovery of lithium from leaching solution

Under the optimal leaching conditions, 60 mL of the leaching solution was analyzed to determine the recovery of Li from the solution. According to the *E*−pH diagram of Li−Fe−P−H_2O system [20], the pH of the leached solution was first adjusted to 6.5 with a 2 mol/L NaOH solution to precipitate the

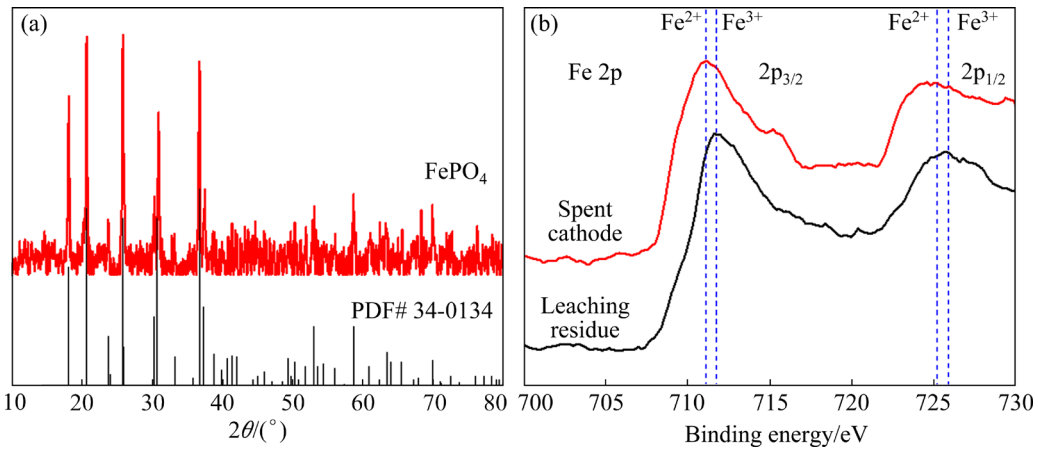

Fig. 4 XRD pattern of leached slag (a); XPS diagram of spent $LiFePO_4$ cathode powder and leaching residue (b)

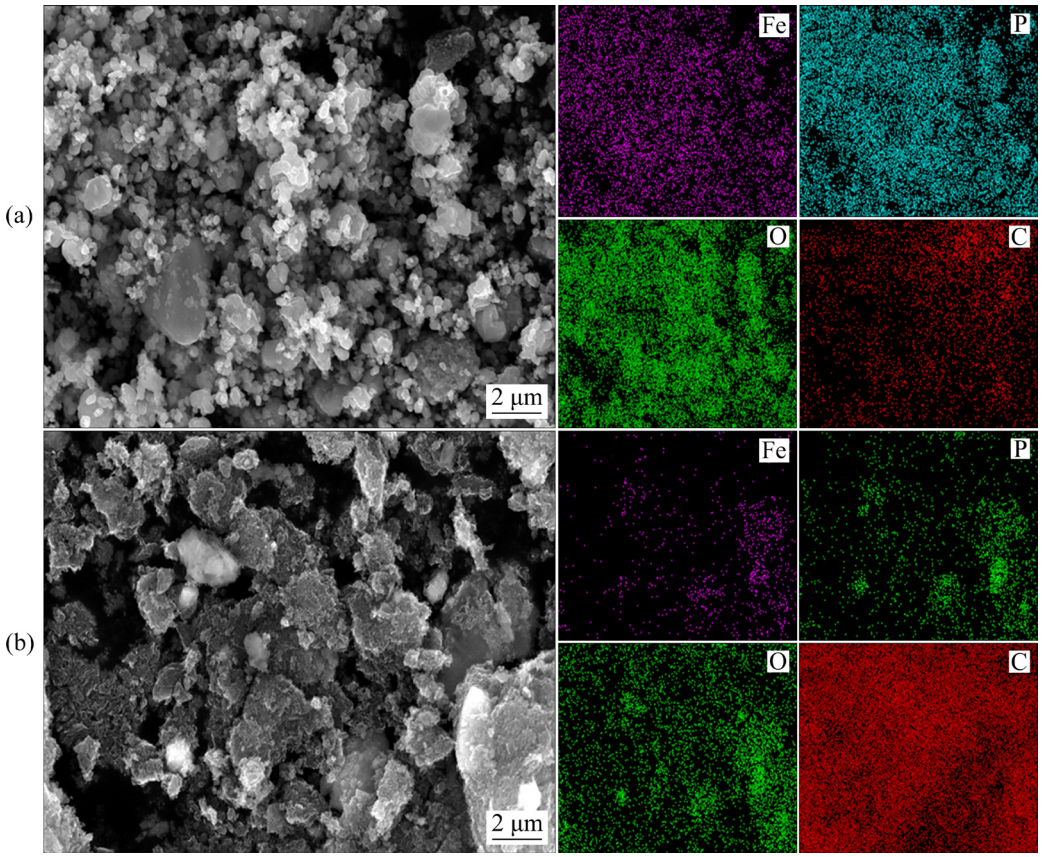

Fig. 5 FE-SEM images and element mappings of spent cathode before (a) and after (b) leaching

Table 1 ICP-OES results of calcined products (wt.%)

Fe	P	Al	Zn	Ni
32.80	18.67	0.0073	0.0003	0.0007

Fe in the form of $Fe(OH)_3$ because the $Fe(OH)_3$ phase is thermodynamically stable under acidic conditions. The results indicated that 90.36% of the Fe precipitated out of solution, while 9% of the Fe remained in solution. The pH was further adjusted to 12.0 using 2 mol/L NaOH, after which 89.6% of the Li precipitated out of solution as Li_3PO_4 at 80 °C. The precipitate was then dried at 100 °C for 12 h and analyzed by XRD (Fig. 6). The XRD pattern of the dried residue was consistent with the standard spectrum of Li_3PO_4 (PDF# 71-1528), and the purity of Li_3PO_4 was determined to be >96.5 wt.% based on ICP-OES. Therefore, the recovered Li_3PO_4 was pure enough to be used to prepare $LiFePO_4$ as a cathode material. It was previously reported that PO_4^{3-} remaining in solution after precipitation of Li could be removed by magnesium-rich engineering carbon [29], suggesting that the chemical precipitation can be used to remove

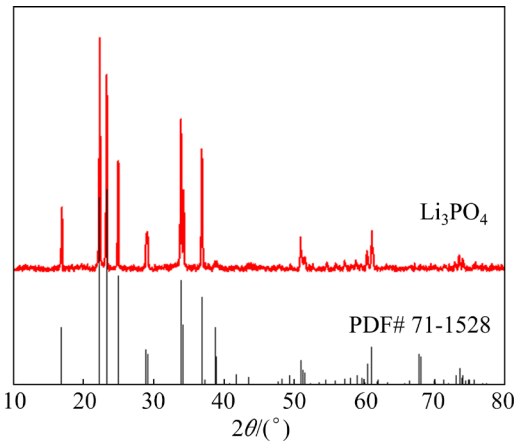

Fig. 6 XRD pattern of in-situ precipitation of Li_3PO_4

phosphorus in the form of insoluble phosphate salts (Reaction (6)):

$$Fe^{3+}+PO_4^{3-}\rightarrow FePO_4\downarrow \quad (6)$$

3.7 Kinetics of lithium leaching

To study the leaching mechanism of Li by pyruvic acid and H_2O_2, the leaching kinetics of Li at different temperatures (25, 40, 60, and 80 °C) was studied according to the hydrometallurgical

principle [9,30]. Figure 7(a) shows the leaching efficiencies of Li at different temperatures and reaction durations. The results showed that the reaction between lithium and pyruvic acid was fast in the initial stage and reached a stable stage soon. The leaching of metals from spent cathode material particles includes the following steps: (1) external diffusion of liquid reactants or products through the liquid boundary layer, (2) internal diffusion of liquid reactants or products through solid product layers, and (3) surface chemical reactions [31,32]. Three types of models are typically used to study leaching kinetics: the diffusion control model (Eq. (7)), surface chemical control model (Eq. (8)), and Avrami equation model (Eq. (9)):

$$1-\frac{2}{3}X-(1-X)^{2/3}=k_a\cdot t \tag{7}$$

$$1-(1-X)^{1/3}=k_b\cdot t \tag{8}$$

$$\ln[-\ln(1-X)]=\ln k_c+n\ln t \tag{9}$$

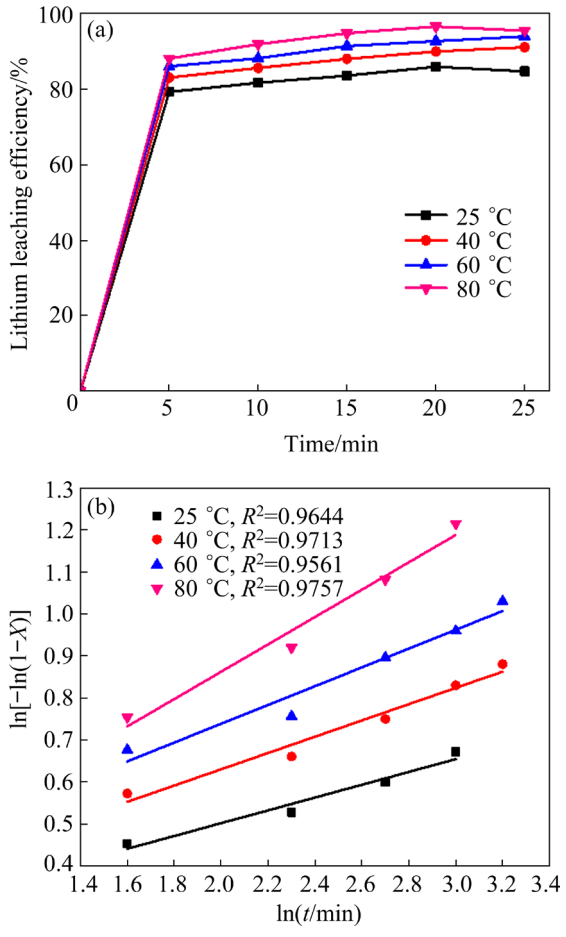

Fig. 7 Leaching efficiency of Li at different temperatures and time (a); Fitting results of Avrami equation at various leaching temperatures for Li (b)

where X is the leaching efficiency of metal at time t (min), k_a is the rate constant controlled by diffusion, k_b is the rate constant controlled by diffusion of the chemical reaction, and k_c is the reaction rate constant (min^{-1}).

The experimental data were substituted into Eqs. (7) and (8) to fit the relationship with time. After fitting the kinetics data to the model in Eqs. (7) and (8), the resulting correlation coefficient of the linear fit was very low, indicating that the model in Eqs. (7)−(8) was not robust enough to fit the data. However, as shown in Fig. 7(a), the leaching efficiency of Li tended to be stable over a long period of time, which was more applicable for the Avrami model (Eq. (9)) than the previous two models [33]. The Avrami equation is often used to describe crystal nucleation and leaching reaction kinetics [34]. Therefore, linear fitting of the Li leaching kinetics data to the Avrami model was performed to determine the Li leaching efficiency at different temperatures (Fig. 7(b)). The results indicated that the model was robust enough to fit the data, with R^2>0.95, demonstrating high correlation.

Based on the rate constant (k_c) and temperature (T) of the reaction, the apparent activation energy (E_a) of the reaction was calculated using the Arrhenius (Eq. (10)) below:

$$k_c=A\exp[-E_a/(RT)] \tag{10}$$

Equation (10) was further transformed into Eq. (11):

$$\ln k_c=\ln\ A-E_a/(RT) \tag{11}$$

where R is the molar gas constant (8.314 $J\cdot K^{-1}\cdot mol^{-1}$), and A is the pre-exponential factor.

The $\ln k$ and $1/T$ data in Fig. 7(b) were fitted by the model shown in Eq. (11), and the results of the fitting are shown in Fig. 8. The correlation of the linear fit (expressed as $\ln k$−$1/T$) was high (R^2=0.9688), indicating that the Avrami model enabled a robust fit of the Li leaching kinetics data. The E_a of the Li leaching process was then calculated to be 11.14 kJ/mol, indicating that the reaction rate was diffusion-limited during the leaching process [35]. The leaching efficiency was proportional to the concentration under the diffusion-limited conditions, and the temperature had less effect on the leaching efficiency than concentration, which was consistent with the experimental results of single factor. The low

activation energy of the Li leaching indicated that the leaching efficiency of Li from the spent $LiFePO_4$ powder was fast, and the pyruvate in the pyruvic acid/H_2O_2 leaching system easily reacted with the Li in the $LiFePO_4$, which was consistent with the thermodynamic data of the leaching process.

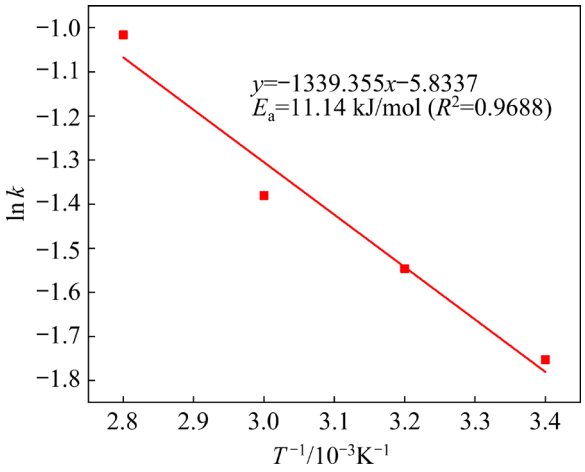

Fig. 8 Arrhenius plot of ln k−1/T

4 Conclusions

(1) The efficiency of a pyruvic acid/H_2O_2 system was explored for the leaching of valuable metals from spent $LiFePO_4$ cathode powder. The optimal conditions of the leaching process to achieve the most efficient leaching of Li comprised a pyruvic acid concentration of 3.0 mol/L, volume of H_2O_2 of 2 mL, solid-to-liquid ratio of 0.1 g/mL, reaction temperature of 80 °C, and reaction time of 20 min.

(2) The leaching residue was calcinated at 600 °C to reduce C content. The Fe/P molar ratio of the calcined leached slag ($FePO_4$) was calculated to be 0.974, which was consistent with the battery-grade $FePO_4$ standards.

(3) The Li was recovered from the leaching solution in the form of Li_3PO_4 via in-situ precipitation with a purity of 96.5 wt.%.

(4) The Gibb's free energy ($\Delta_rG^{\ominus}$) of the entire leaching process was −73.89 kJ/mol, indicating that the reaction is favorable and energy-yielding. Furthermore, the apparent activation energy (E_a) of the lithium leaching process was 11.14 kJ/mol.

CRediT authorship contribution statement

Ya-hui WANG: Conceptualization, Methodology, Formal analysis, Investigation, Writing – Original draft; **Ji-jun WU:** Conceptualization, Resources, Supervision, Project administration, Funding acquisition, Writing – Review & editing; **Guo-chen HU:** Validation, Data curation; **Wen-hui MA:** Resources, Supervision, Project administration, Funding acquisition.

Declaration of competing interest

The authors declare that they have no known competing financial interests or personal relationships that could have appeared to influence the work reported in this paper.

Acknowledgments

The authors wish to acknowledge the financial support on this research from the Talent Training Program of Yunnan Province, China (No. 202005AC160041) and the Major R&D Project of Yunnan Province of China (No. 202002AB0800020102).

References

[1] ZUO Wen-chao, LI Yue-qing, WANG Yu-hong. Research on the optimization of new energy vehicle industry research and development subsidy about generic technology based on the three-way decisions [J]. Journal of Cleaner Production, 2019, 212: 46−55.

[2] LI Jian-zhong. Charging Chinese future: The roadmap of China's policy for new energy automotive industry [J]. International Journal of Hydrogen Energy, 2020, 45: 11409−11423.

[3] EI GHOSSEIN N, SARI A, VENET P. Effects of the hybrid composition of commercial lithium-ion capacitors on their floating aging [J]. IEEE Transactions on Power Electronics, 2019, 34: 2292−2299.

[4] ZHENG Xiao-hong, ZHU Ze-wen, LIN Xiao, ZHANG Yi, HE Yi, CAO Hong-bin, SUN Zhi. A mini-review on metal recycling from spent lithium ion batteries [J]. Engineering, 2018, 4: 361−370.

[5] GARCIA E M, SANTOS J S, PEREIRA E C, FREITAS M B J G. Electrodeposition of cobalt from spent Li-ion battery cathodes by the electrochemistry quartz crystal microbalance technique [J]. Journal of Power Sources, 2008, 185: 549−553.

[6] BYEON P, BIN BAE H, CHUNG H S, LEE S G, KIM J G, LEE H J, CHOI J W, CHUNG S Y. Atomic-scale observation of $LiFePO_4$ and $LiCoO_2$ dissolution behavior in aqueous solutions [J]. Advanced Functional Materials, 2018, 28: 1−10.

[7] YADAV P, JIE C J, TAN S, SRINIVASAN M. Recycling of cathode from spent lithium iron phosphate batteries [J]. Journal of Hazardous Materials, 2020, 399: 123068.

[8] DOS SANTOS C S, ALVES J C, DA SILVA S P, SITA L E, DA SILVA P R C, DE ALMEIDA L C, SCARMINIO J. A closed-loop process to recover Li and Co compounds and to

resynthesize $LiCoO_2$ from spent mobile phone batteries [J]. Journal of Hazardous Materials, 2018, 362: 458−466.

[9] MENG Qi, ZHANG Ying-jie, DONG Peng. A combined process for cobalt recovering and cathode material regeneration from spent $LiCoO_2$ batteries: Process optimization and kinetics aspects [J]. Waste Management, 2017, 71: 372−380.

[10] ZHAO Yan-lan, YUAN Xing-zhong, JIANG Long-bo, WEN Jia, WANG Hou, GUAN Ren-peng, ZHANG Jing-jing, ZENG Guang-ming. Regeneration and reutilization of cathode materials from spent lithium-ion batteries [J]. Chemical Engineering Journal, 2019, 383: 123089.

[11] LIU Chun-wei, LIN Jiao, CAO Hong-bin, ZHANG Yi, SUN Zhi. Recycling of spent lithium-ion batteries in view of lithium recovery: A critical review [J]. Journal of Cleaner Production, 2019, 228: 801−813.

[12] GEORGI-MASCHLER T, FRIEDRICH B, WEYHE R, HEEGN H, RUTZ M. Development of a recycling process for Li-ion batteries [J]. Journal of Power Sources, 2012, 207: 173−182.

[13] SHIN S M, KIM N H, SOHN J S, YANG D H, KIM Y H. Development of a metal recovery process from Li-ion battery wastes [J]. Hydrometallurgy, 2005, 79: 172−181.

[14] LI Huan, XING Sheng-zhou, LIU Yu, LI Fu-jie, GUO Hui, KUANG Ge. Recovery of lithium, iron, and phosphorus from spent $LiFePO_4$ batteries using stoichiometric sulfuric acid leaching system [J]. ACS Sustainable Chemistry & Engineering, 2017, 5: 8017−8024.

[15] YANG Yong-xia, ZHENG Xiao-hong, CAO Hong-bin, ZHAO Chun-long, LIN Xiao, NING Peng-ge, ZHANG Yi, JIN Wei, SUN Zhi. A closed-loop process for selective metal recovery from spent lithium iron phosphate batteries through mechanochemical activation [J]. ACS Sustainable Chemistry & Engineering, 2017, 5: 9972−9980.

[16] SHIN E J, KIM S, NOH J K, BYUN D, CHUNG K Y, KIM H S, CHO B W. A green recycling process designed for $LiFePO_4$ cathode materials for Li-ion batteries [J]. Journal of Materials Chemistry A, 2015, 3: 11493−11502.

[17] MAHANDRA H, GHAHREMAN A. A sustainable process for selective recovery of lithium as lithium phosphate from spent $LiFePO_4$ batteries [J]. Resources Conservation and Recycling, 2021, 175: 105883.

[18] YANG Yong-xia, MENG Xiang-qi, CAO Hong-bin, LIN Xiao, LIU Chen-ming, SUN Yong, ZHANG Yi, SUN Zhi. Selective recovery of lithium from spent lithium iron phosphate batteries: A sustainable process [J]. Green Chemistry, 2018, 20: 3121−3133.

[19] FAN Er-sha, LI Li, ZHANG Xiao-xiao, BIAN Yi-fan, XUE Qing, WU Jia-wei, WU Feng, CHEN Ren-jie. Selective recovery of Li and Fe from spent lithium-ion batteries by an environmentally friendly mechanochemical approach [J]. ACS Sustainable Chemistry & Engineering, 2018, 6: 11029−11035.

[20] SHENTU Hua-jian, XIANG Bo, CHENG Ya-jun, DONG Tao, GAO Jie, XIA Yong-gao. A fast and efficient method for selective extraction of lithium from spent lithium iron phosphate battery [J]. Environmental Technology & Innovation, 2021, 23: 101569.

[21] RAMANA C V, MAUGER A, GENDRON F, JULIEN C M, ZAGHIB K. Study of the Li-insertion/extraction process in $LiFePO_4/FePO_4$ [J]. Journal of Power Sources, 2009, 187: 555−564.

[22] LI Li, QU Wen-jie, ZHANG Xiao-xiao, LU Jun, CHEN Ren-jie, WU Feng, AMINE K. Succinic acid-based leaching system: A sustainable process for recovery of valuable metals from spent Li-ion batteries [J]. Journal of Power Sources, 2015, 282: 544−551.

[23] JHA M K, KUMARI A, JHA A K, KUMAR V, HAIT J, PANDEY B D. Recovery of lithium and cobalt from waste lithium ion batteries of mobile phone [J]. Waste Management, 2013, 33: 1890−1897.

[24] LI Li, LU Jun, REN Yang, ZHANG Xiao-xiao, CHEN Ren-jie, WU Feng, AMINE K. Ascorbic-acid-assisted recovery of cobalt and lithium from spent Li-ion batteries [J]. Journal of Power Sources, 2012, 218: 21−27.

[25] BEHERA S S, PARHI P K. Leaching kinetics study of neodymium from the scrap magnet using acetic acid [J]. Separation and Purification Technology, 2016, 160: 59−66.

[26] CHURIKOV A V, IVANISHCHEV A V, USHAKOV A V, GAMAYUNOVA I M, LEENSON I A. Thermodynamics of $LiFePO_4$ solid-phase synthesis using iron(II) oxalate and ammonium dihydrophosphate as precursors [J]. Journal of Chemical and Engineering Data, 2013, 58: 1747−1759.

[27] CASTRO L, DEDRYVERE R, EI KHALIFI M, LIPPENS P E, BREGER J, TESSIER C, GONBEAU D. The spin-polarized electronic structure of $LiFePO_4$ and $FePO_4$ evidenced by in-lab XPS [J]. Journal of Physical Chemistry C, 2010, 114: 17995−18000.

[28] WU De-you, WANG Dong-xing, LIU Zhi-qiang, RAO Shuai, ZHANG Kui-fang. Selective recovery of lithium from spent lithium iron phosphate batteries using oxidation pressure sulfuric acid leaching system [J]. Transactions of Nonferrous Metals Society of China, 2022, 32: 2071−2079.

[29] ZHANG Yan, GUO Xing-ming, YAO Ying, WU Feng, ZHANG Cun-zhong, CHEN Ren-jie, LU Jun, AMINE K. Mg-enriched engineered carbon from lithium-ion battery anode for phosphate removal [J]. ACS Applied Materials & Interfaces, 2016, 8: 2905−2909.

[30] LI Li, BIAN Yi-fan, ZHANG Xiao-xiao, GUAN Yi-biao, FAN Er-sha, WU Feng, CHEN Ren-jie. Process for recycling mixed-cathode materials from spent lithium-ion batteries and kinetics of leaching [J]. Waste Management, 2017, 71: 362−371.

[31] MESHRAM P, PANDEY B D, MANKHAND T R. Process optimization and kinetics for leaching of rare earth metals from the spent Ni-metal hydride batteries [J]. Waste Management, 2016, 51: 196−203.

[32] MESHRAM P, PANDEY B D, MANKHAND T R. Leaching of base metals from spent Ni-metal hydride batteries with emphasis on kinetics and characterization [J]. Hydrometallurgy, 2015, 158: 172−179.

[33] TRAN T H, GOVIN A, GUYONNET R, GROSSEAU P, LORS C, DAMIDOT D, DEVES O, RUOT B. Avrami's law based kinetic modeling of colonization of mortar surface by alga *Klebsormidium flaccidum* [J]. International Biodeterioration & Biodegradation, 2013, 79: 73−80.

[34] YANG Qun, LI Qi, ZHANG Guo-fan, SHI Qing, FENG

Hai-gang. Investigation of leaching kinetics of aluminum extraction from secondary aluminum dross with use of hydrochloric acid [J]. Hydrometallurgy, 2019, 187: 158−167.
[35] GAO Wen-fang, ZHANG Xi-hua, ZHENG Xiao-hong, LIN Xiao, CAO Hong-bin, ZHANG Yi, SUN Zhi. Lithium carbonate recovery from cathode scrap of spent lithium-ion battery—A closed-loop process [J]. Environmental Science & Technology, 2017, 51: 1662−1669

利用有机酸浸出系统从废旧磷酸铁锂中回收 Li 和 Fe

王亚辉[1]，伍继君[1,2]，胡国琛[1]，马文会[1,2]

1．昆明理工大学 冶金与能源工程学院，昆明 650093；
2．昆明理工大学 真空冶金国家工程实验室，昆明 650093

摘　要：采用湿法冶金从废旧 $LiFePO_4$ 正极粉末中回收有价金属锂和铁，回收产物作为原料制备磷酸铁锂。通过优化浸出工艺参数，在丙酮酸浓度为 3.0 mol/L、H_2O_2 体积为 2 mL、固液比为 0.1 g/mL、反应温度为 80 ℃以及反应时间为 20 min 的条件下，Li 的浸出效率达到 96.56%。采用 XRD、XPS、FE-SEM 和 EDS 对浸出残渣进行表征。结果表明，浸出残渣为 $FePO_4$，Fe/P 摩尔比为 0.974。将浸出液的 pH 值调整到 12.0，并在 80 ℃搅拌 2 h 后，浸出液中的 Li 通过原位沉淀以 Li_3PO_4 形式回收，其纯度为 96.5% (质量分数)。丙酮酸/H_2O_2 溶液浸出 Li 的反应动力学数据符合 Avrami 模型(R^2>0.95)。Li 浸出过程的活化能较低，表明扩散限制浸出过程中的反应速率。

关键词：废旧磷酸铁锂；丙酮酸；浸出动力学；Avrami 模型；锂离子电池

(Edited by Bing YANG)